# High-Precision Ramsey-Comb Spectroscopy Based on High-Harmonic Generation

L. S. Dreissen, C. Roth, E. L. Gründeman, J. J. Krauth, M. Favier, and K. S. E. Eikema*
*LaserLaB, Department of Physics and Astronomy, Vrije Universiteit, De Boelelaan 1081, 1081 HV Amsterdam, Netherlands*

(Received 17 May 2019; published 2 October 2019)

High-harmonic generation (HHG) is widely used for up-conversion of amplified (near) infrared ultrafast laser pulses to short wavelengths. We demonstrate that Ramsey-comb spectroscopy, based on two such pulses derived from a frequency-comb laser, enables us to observe phase effects in this process with a few mrad precision. As a result, we could perform the most accurate spectroscopic measurement based on light from HHG, illustrated with a determination of the $5p^6 \rightarrow 5p^5 8s^2[3/2]_1$ transition at 110 nm in $^{132}$Xe. We improve its relative accuracy $10^4$ times to a value of $2.3 \times 10^{-10}$. This is 3.6 times better than shown before involving HHG, and promising to enable $1S$-$2S$ spectroscopy of $He^+$ for fundamental tests.

DOI: 10.1103/PhysRevLett.123.143001

High-precision spectroscopy in calculable atomic and molecular systems is at the heart of the most precise tests of bound-state quantum electrodynamics (QED) and searches for new physics beyond the standard model [1–6]. Instrumental in this development was the invention of the optical frequency comb (FC) [7,8] which enables precise optical frequency measurements referenced to an atomic clock. However, uncertainties in finite nuclear-size effects are hampering further progress [9]. Instead, spectroscopy has been used to measure the proton size in atomic and muonic hydrogen, but with partly conflicting results [10–16]. High-precision spectroscopy of the $1S$-$2S$ transition in $He^+$ would provide new possibilities for fundamental tests as the uncertainty there is less dominated by nuclear size effects [17]. Combined with muonic $He^+$ spectroscopy [18,19] one can extract, e.g., the alpha particle radius or the Rydberg constant. A major experimental challenge arises from the requirement of extreme ultraviolet (XUV) light at 60 nm (or shorter), to excite the transition. A similar challenge exists for spectroscopy of highly-charged ions [5], or the Thorium nuclear clock transition near 150 nm in the vacuum ultraviolet (VUV) [20,21]. At those wavelengths a relative accuracy of 0.1 ppm has been achieved with Fourier-transform spectroscopy techniques [22], and 0.03 ppm with low harmonics from nanosecond pulsed lasers [23]. A higher accuracy can be reached with light from high-harmonic generation (HHG), induced by focusing ultrafast high-energy laser pulses in a noble gas at intensities of $\sim 10^{14}$ W/cm$^2$. The process can be understood using the three-step model [24,25], involving tunnel ionization and recollision of an electron. This highly coherent process leads to the generation of a series of odd harmonics, which are tightly linked to the fundamental wave [26–30]. In combination with frequency-comb lasers, it has been used to achieve a spectroscopic accuracy of about 1 ppb at VUV and XUV wavelengths [31,32].

To improve on this we recently developed the Ramsey-comb spectroscopy (RCS) method [33,34], based on pairs of powerful amplified FC pulses in a Ramsey-type [35] excitation scheme. Using only two pulses can compromise the accuracy provided by the FC laser [31], but the differential nature of RCS leads to the recovery of this accuracy [33] and also to a strong suppression of the influence of the ac-Stark (light) shift. Other advantages of RCS compared to spectroscopy using cavity-based FC up-conversion [28–30] include easy tunability, simple up-conversion in a gas jet (no resonator required), a high excitation probability, and a nearly 100% detection efficiency. RCS has been demonstrated successfully at wavelengths ranging from the near-infrared (NIR) [33], to the deep ultraviolet, using low-order nonlinear up-conversion in crystals [36,37].

Extending RCS to shorter wavelengths with HHG is not trivial because a dynamic plasma is produced in HHG. This can lead to a reduced HHG yield and a time-dependent influence on the phase (and phase-matching) of the generated harmonics [38–40], and therefore errors in the extracted transition frequency. Plasma effects in HHG have been investigated at picosecond timescales, showing a nearly instantaneous response based on electron dynamics [41,42], but not at longer timescales relevant for precision spectroscopy.

In this Letter we show that the phase evolution of an atomic excitation obtained from RCS can be used to investigate the phase influence of plasma formation in HHG. We can monitor this on a nanosecond timescale and with mrad phase sensitivity. The results obtained at 110 nm (the seventh harmonic of 770 nm) show that most of the phase effects are caused by free electrons in the plasma and therefore strongly decrease within a few nanoseconds. Under the right conditions, the effects can be made negligibly small, enabling spectroscopy with unprecedented

 

accuracy using radiation from HHG. This is demonstrated with a measurement of the $5p^6 \rightarrow 5p^5 8s^2[3/2]_1$ transition in xenon with a relative accuracy of $2.3 \times 10^{-10}$.

Ramsey-comb spectroscopy [33,34] requires phase and time-controlled laser pulses. The output of a FC laser [7,8] is the ideal source for this as both the repetition time $T_{\mathrm{rep}}$ and carrier-envelope phase evolution $\Delta\phi_{\mathrm{ceo}}$ of the pulses can be referenced to an atomic clock. For two pulses that are resonant with a two-level system at a transition frequency $f_{\mathrm{tr}}$, each excitation pulse can be thought to induce a superposition of the ground and excited state. These contributions interfere depending on the phase evolution $2\pi f_{\mathrm{tr}}\Delta t$ of the superposition state (where $\Delta t$ is the pulse delay) and the phase difference $\Delta\phi$ between the two laser pulses (which includes $\Delta\phi_{\mathrm{ceo}}$). The excited state population after the second laser pulse can be written as $|c_e(\Delta t, \Delta\phi)|^2 \propto \cos(2\pi f_{\mathrm{tr}}\Delta t + \Delta\phi)$. When a scan of $T_{\mathrm{rep}}$ is made on a femtosecond or attosecond timescale, the effect of the phase evolution on $|c_e|^2$ can be observed in the form of a Ramsey fringe. A series of these fringes can be obtained at different multiples of the repetition time ($\Delta N \times T_{\mathrm{rep}}$) by selecting different pairs of pulses. The transition frequency is then extracted from the phase *difference* between these Ramsey fringes [34], which leads to a cancellation of any induced, but constant, phase shift. This includes the optical phase shift between the two pulses (e.g., from amplification), but also the ac-Stark light shift of the energy levels for a constant pulse energy [37].

The starting point of the laser system is a mode-locked Ti:sapphire FC laser ($T_{\mathrm{rep}} = 7.9$ ns) which is referenced to a Cs atomic clock (Symmetricon CsIII 4310B). The pulses are spectrally filtered within a 4*f*-grating stretcher to a bandwidth of 8–10 nm centered around 770 nm to avoid excitation of neighboring transitions.

A noncollinear Optical Parametric Chirped Pulse Amplifier (NOPCPA), based on 3 beta-barium borate (BBO) crystals, is used to selectively amplify two of the FC pulses. The delay between these pulses is an integer multiple of $T_{\mathrm{rep}}$ and depends on the settings of a home-built double-pulse pump laser at 532 nm [43,44]. A typical energy of 2 mJ/pulse is reached after recompression to a ~220 fs pulse length. HHG is performed (see Fig. 1) by focusing ($f = 25$ cm) the beam (4 mm FWHM diameter) in an argon gas jet. A central beam block of 1 mm diameter is used to convert the intensity profile of the fundamental beam into a donutlike shape before HHG. This enables efficient separation of the fundamental and harmonic beam with an adjustable iris after HHG, because the harmonics travel on axis and with a much lower divergence than the fundamental beam. A LiF plate blocks harmonics with $\lambda < 105$ nm, while the seventh harmonic at 110 nm is transmitted with an efficiency of 40%. The beam is subsequently refocused using a pair of grazing-incidence gold-coated toroidal mirrors, acting as a 1:1 telescope. The refocused VUV beam is crossed at 90° with a pulsed supersonic beam of xenon (backing pressure 500 mbar, pulse length ≈40 $\mu$s). Excited atoms are detected by state selective ionization with a 3 mJ pulse at 1064 nm, and the resulting ions are recorded isotope selectively with a time-of-flight mass separator. Despite previous reports of Xe cluster formation in supersonic expansions [45,46], no evidence for it was found in our experiment, even after many tests with different skimmers and valves.

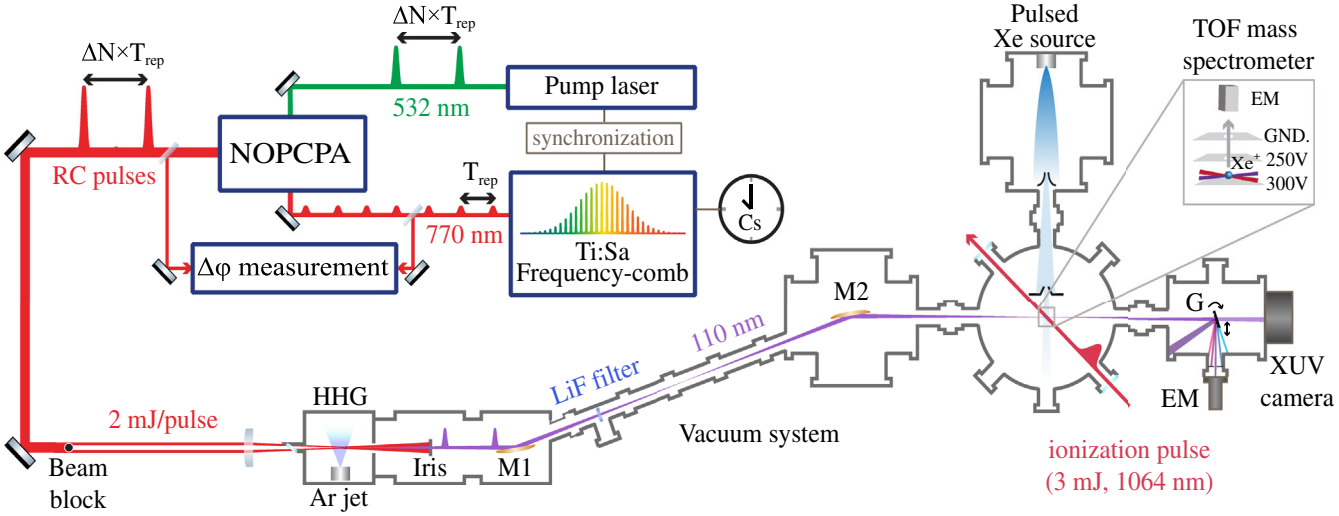


FIG. 1. Schematic of the HHG-RCS setup. A pair of pulses from a Ti:Sa FC laser is selectively amplified at different multiples of the repetition time ($\Delta N \times T_{\mathrm{rep}}$) in a NOPCPA. They are up-converted using HHG in an argon jet (shown 90° rotated). The seventh harmonic is refocused using a pair of toroidal mirrors ($M1$ and $M2$) at grazing incidence. Xenon atoms from a pulsed source are excited at 90° angle to reduce the first-order Doppler effect. An ionization pulse at 1064 nm is delayed by 2 ns with respect to the last excitation pulse and selectively ionizes the excited atoms. After pulsed field extraction, the ions are detected with an ETP AF880 electron multiplier (EM) at the end of a 47 cm long time-of-flight (TOF) drift tube. $G$ = grating (3600 lines/mm).

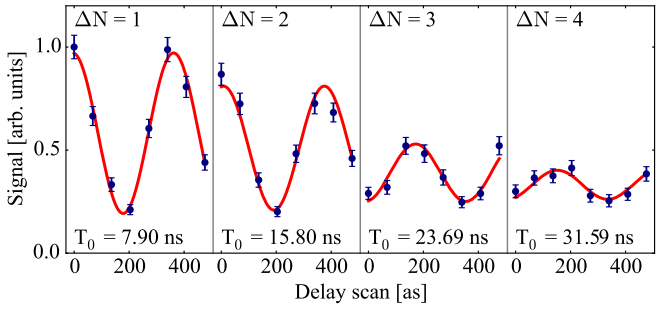


FIG. 2. Typical Ramsey-comb scan of the $5p^6 \rightarrow 5p^5 8s^2[3/2]_1$ transition at 110 nm in $^{132}$Xe. $\Delta N$ refers to the interpulse delay in multiples of $T_{\mathrm{rep}} = 7.9$ ns of the FC and $T_0$ indicates the initial delay. The individual data points are obtained by averaging over 700 laser shots, which leads to a measurement time of 3.3 min/fringe. The fringes are fitted with a fixed frequency to determine their phase.

A typical RCS scan of $^{132}$Xe with $\Delta N = 1$–4 is shown in Fig. 2. Most measurements were done with only a pair of Ramsey fringes (e.g., $\Delta N = 2$ and $\Delta N = 4$), taking just 6.6 minutes, to minimize the influence of possible drifts. For the same reason, the data points were recorded in random order and sorted according to pulse delay afterwards, instead of a sequential scan as was done in previous RCS experiments.

The contrast of the Ramsey fringes (80%–90% for $\Delta N = 1$) decreases notably as a function of $\Delta N$. This is partly caused by the limited upper-state lifetime of ≈22 ns [47], Doppler effects, and a 50–70 mrad rms phase noise of the amplified FC pulses. However, the decay of contrast was dominated by the limited transit time of the xenon atoms through the focused VUV beam. Therefore astigmatism was introduced to increase the interaction time from 16 ns (focus diameter 15 $\mu$m) to 32 ns (30 $\mu$m) at the expense of a maximum local wave front tilt of ≈1.5 mrad. This was inferred from the fundamental beam profile in the focal plane.

The combination of HHG with the refocusing optics revealed a subtle but interesting effect originating from the NOPCPA. An intensity (and alignment) dependent spatial walk-off induced effect led to a slight difference in beam pointing (<0.5 mrad) between the two amplified pulses. This reduced the overlap between the two refocused VUV pulses and further limited the interaction time with the atoms. It also led to a strong, initially unexplained, day-to-day variation of Ramsey signal contrast. After implementation of a walk-off compensating configuration [48] in the first two passes of the amplifier, the beam pointing difference was reduced to below 20 $\mu$rad. This was a crucial step to be able to combine HHG with RCS. In previous RCS experiments with low harmonics in crystals [33,36,37], the walk-off induced beam pointing difference had little effect and went unnoticed because mm-size, collimated beams could be used.

With the aforementioned improvements, the influence of the generated plasma in the HHG process on the phase of the VUV light could be measured. For this we

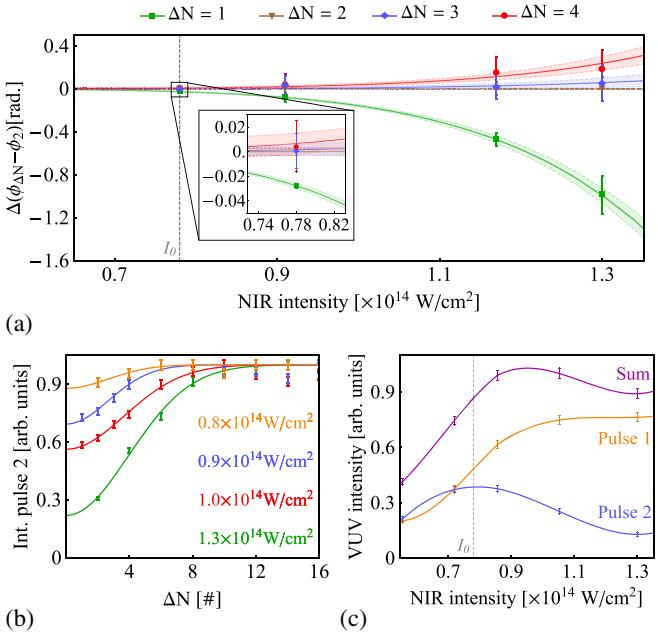


FIG. 3. The influence of plasma-induced effects from HHG on the phase and the intensity of the second VUV pulse. (a) The phase difference between $\Delta N = 2$ (reference) and $\Delta N = 1$, 3 and 4 as function of driving intensity. The data are fitted with $\phi \propto I^7$ and the shaded area indicates the $1\sigma$ uncertainty. The dashed line shows the intensity $I_0$ at normal operation and the inset shows a zoom-in at this value. (b) The intensity of the second VUV pulse as a function of delay for different driving intensities. (c) The harmonic yield of the two pulses and their sum as a function of driving intensity. The lines connecting the data points are splines to guide the eye.

investigated the phase dependence of the Ramsey fringes on different conditions in the HHG process.

In Fig. 3(a) the phase at $\Delta N = 1$, 3, and 4 relative to $\Delta N = 2$ as a function of the driving intensity is shown. This intensity was determined from the measured pulse energy, beam waist, and pulse length (using frequency-resolved optical gating). We have chosen the phase at $\Delta N = 2$ as a reference, because the dynamics changes markedly at this delay (15.8 ns) and the signal quality was better than for the larger delays. The observed phase shift as a function of the intensity shows a near-exact seventh-order dependence [see fitted curves in Fig. 3(a)]. At $\Delta N = 1$, a maximum phase shift of 1 rad is observed. This is reduced by an order of magnitude at larger pulse delays, from which we conclude that the phase shift, especially at $\Delta N = 1$, is dominated by the influence of fast moving free electrons (leaving the interaction zone on a ps to few ns time scale). As the atoms and ions move much slower, their contribution is seen mostly at later times.

This difference in dynamics between slow atoms (ions), and fast electrons is also illustrated in Fig. 3(b), which shows the relative intensity of the second VUV pulse as a function of delay. The yield is significantly reduced up to 70% for high driving intensity because up-conversion of

the first pulse leads to a significant depletion of neutral atoms. Note that this also leads to a reduction in contrast of the Ramsey fringes due to the imbalance between the two excitation contributions, and therefore a larger uncertainty for the phase [Fig. 3(a)]. The intensity of the second VUV pulse revives to a similar level as the first in 50–100 ns, depending on the driving intensity. This is in agreement with the expected transit time of argon atoms ($v \approx$ 500 m/s) through the focus (50 $\mu$m) and it is much slower than the observed electron dynamics.

These results show that RCS can be combined successfully with HHG for precision measurements at short wavelengths. To demonstrate this we made an absolute calibration of the probed transition. Most of the observed phase effects occur at short pulse delays, and therefore only Ramsey fringes from $\Delta N = 2$ or higher were used to determine the transition frequency. In addition, the driving intensity was moderated to $I_0 = 0.78 \times 10^{14}$ W/cm$^2$ [the dashed line in Figs. 3(a) and 3(b)]. The remaining shift in this case is $-2(5)$ mrad between $\Delta N = 2$ and $\Delta N = 3$ and $-7(9)$ mrad between $\Delta N = 2$ and $\Delta N = 4$ [inset in Fig. 3(a)]. This corresponds to a shift of $-32(91)$ kHz and $-67(86)$ kHz, respectively, of the extracted transition frequency and is consistent with zero within the uncertainty. Only a small penalty of 15%–20% of the maximum VUV yield (the sum of pulse 1 and 2) is paid by reducing the fundamental intensity [Fig. 3(c)]. The influence of the adiabatic HHG phase shift [25], which depends on the driving NIR intensity, is suppressed in RCS, similar to ac-Stark shift. It is estimated to be below a few mrad (<30 kHz) in the VUV for an energy stability of <0.2% in the NIR. The phase stability of the fundamental pulses is measured using spectral interferometry (see Ref. [44]) and found to be constant well within 1 mrad at 770 nm. The corresponding frequency uncertainty is 140 kHz in the VUV.

The RCS signal is repetitive and leads to a frequency ambiguity of multiples of $f_{\mathrm{rep}} = 1/T_{\mathrm{rep}}$ [31]. Therefore the measurements have been repeated with three slightly different values of $T_{\mathrm{rep}}$ to obtain a single transition frequency with 99.2% confidence over a $4\sigma$ range of the former measurements [49].

After the identification of the transition frequency, several systematic effects were investigated. The largest one was the Doppler effect, which was quantified and reduced by comparing the transition frequency obtained from pure xenon [velocity of 285(30) m/s] with that from a 3:1 Ar:Xe mixture [480(30) m/s]. The angle between the atomic and the VUV beam was adjusted to minimize the observed frequency difference to a few MHz, after which the Doppler-free transition frequency was determined by extrapolation to zero velocity. In total, 300 measurements have been performed and the result is shown in Fig. 4. Besides the Doppler effect, RCS is also affected by the recoil shift due to the absorption of a single photon [50]. This is accounted for by applying a correction of 125 kHz.

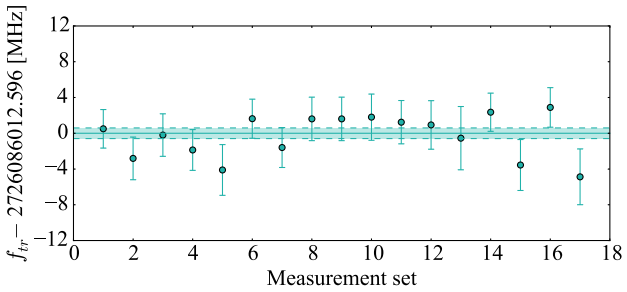


FIG. 4. The Doppler-free transition frequency of the $5p^6 \rightarrow 5p^5 8s^2[3/2]_1$ transition in $^{132}$Xe at 110 nm. Each data point is based on ten measurements at two different speeds of xenon. The blue shaded area indicates the $1\sigma$ uncertainty.

The RCS method strongly suppresses the influence of ac-Stark shifts [36,37]. Measurements at different intensity levels were done to check for a residual effect, leading to an uncertainty of 20 kHz from the NIR light (estimated at $1 \times 10^{11}$ W/cm$^2$) and 85 kHz from the VUV intensity (estimated at $5 \times 10^7$ W/cm$^2$). The dc-Stark shift and Zeeman shift were reduced by exciting in a field-compensated environment. An additional uncertainty of 20 kHz and 52 kHz, respectively, is taken into account for the possible influence of residual stray fields.

The final result of the $5p^6 \rightarrow 5p^5 8s^2[3/2]_1$ transition frequency in $^{132}$Xe has a total accuracy of 630 kHz and the value together with the corrections and error budget is listed in Table I.

To conclude, we demonstrated the first RCS measurement in combination with HHG. It enables extending RCS to much shorter wavelengths than what is possible with nonlinear crystals [36,37]. However, HHG is also known to introduce detrimental phase shifts from plasma formation. These effects have been investigated with RCS using xenon atoms as a phase detector, leading to mrad-level sensitivity. We are able to discriminate between two effects which originate from different aspects of plasma formation. The intensity of the generated light is predominantly influenced by the depletion of neutral atoms. This effect persists for

TABLE I. Contributions (in kHz) to the measurement of the $5p^6 \rightarrow 5p^5 8s^2[3/2]_1$ transition frequency in xenon.

| | Value or correction | $(1\sigma)$ |
|---|---|---|
| Doppler-free transition frequency | 2 726 086 012 596 | (600)[a] |
| Light induced effects | 0 | (87) |
| dc-Stark shift | 0 | (20) |
| Zeeman shift | 0 | (52) |
| Amplifier phase shift | 0 | (140) |
| Recoil shift | −125 | $(10^{-7})$ |
| Total | 2 726 086 012 471 | (630) |

[a]Including the uncertainty of ≈90 kHz due to the residual HHG phase shift (see text) and the correction for the second-order Doppler shift of 1.2 kHz for pure Xe and 3.5 kHz for the mixture.

relatively long pulse delays (50–100 ns), because it depends on the dynamics of neutral atoms in a gas jet. On the other hand, the phase of the generated light is mainly affected by the dispersion from the generated free electrons. As these electrons move faster than the atoms, a significant reduction of this effect is already observed at 16 ns, which enables RCS on the $5p^6 \rightarrow 5p^5 8s^2[3/2]_1$ transition in xenon at 110 nm with a sub-MHz accuracy.

The obtained transition frequency is in good agreement with the previous determination [49], but improves upon it by a factor $10^4$. With this measurement an unprecedented fractional uncertainty of $2.3 \times 10^{-10}$ is achieved using light obtained with HHG.

The HHG process contributes remarkably little to the error budget of the frequency determination (Table I). The only reason that previous RCS experiments [33,36,37] without HHG reached a higher accuracy was the longer pulse delay that could be applied in those cases. The short maximum transit time of 32 ns (and therefore pulse delay) in the current experiment is caused by the tight focus of the harmonic beam, because the setup has been designed for $1S$-$2S$ spectroscopy of a single trapped $He^+$ ion. This limited the accuracy for xenon as the influence of most systematic errors reduce proportionally to the pulse delay. Fortunately, future targets, such as $He^+$, can be trapped and observed for much longer times. Then pulse delays in the microsecond range can be used, with the added benefit that HHG phase effects are then effectively zero, even at high levels of ionization. This makes RCS very promising for precision measurements with (sub)kHz-level accuracy at VUV and XUV wavelengths.

We thank Professor Dr. Frédéric Merkt for valuable discussions during this experiment. K. E. acknowledges the European Research Council for an ERC-Advanced grant under the European Union's Horizon 2020 research and innovation programme (Grant Agreement No. 695677) and FOM/NWO for a Program Grant (16MYSTP).

*Corresponding author.
k.s.e.eikema@vu.nl

[1] C. G. Parthey *et al.*, Improved Measurement of the Hydrogen $1S - 2S$ Transition Frequency, Phys. Rev. Lett. **107**, 203001 (2011).

[2] N. Hölsch, M. Beyer, E. J. Salumbides, K. S. E. Eikema, W. Ubachs, C. Jungen, and F. Merkt, Benchmarking Theory with an Improved Measurement of the Ionization and Dissociation Energies of $H_2$, Phys. Rev. Lett. **122**, 103002 (2019).

[3] J. Biesheuvel, J.-P. Karr, L. Hilico, K. S. E. Eikema, W. Ubachs, and J. C. J. Koelemeij, Probing QED and fundamental constants through laser spectroscopy of vibrational transitions in $HD^+$, Nat. Commun. **7**, 10385 (2016).

[4] T. Stöhlker *et al.*, $1s$ Lamb Shift in Hydrogenlike Uranium Measured on Cooled, Decelerated Ion Beams, Phys. Rev. Lett. **85**, 3109 (2000).

[5] M. G. Kozlov, M. S. Safronova, J. R. Crespo López-Urrutia, and P. O. Schmidt, Highly charged ions: Optical clocks and applications in fundamental physics, Rev. Mod. Phys. **90**, 045005 (2018).

[6] I. Draganić, J. R. Crespo López-Urrutia, R. DuBois, S. Fritzsche, V. M. Shabaev, R. S. Orts, I. I. Tupitsyn, Y. Zou, and J. Ullrich, High Precision Wavelength Measurements of QED-Sensitive Forbidden Transitions in Highly Charged Argon Ions, Phys. Rev. Lett. **91**, 183001 (2003).

[7] R. Holzwarth, T. Udem, T. W. Hänsch, J. C. Knight, W. J. Wadsworth, and P. S. J. Russell, Optical Frequency Synthesizer for Precision Spectroscopy, Phys. Rev. Lett. **85**, 2264 (2000).

[8] D. J. Jones, S. A. Diddams, J. K. Ranka, A. Stentz, R. S. Windeler, J. L. Hall, and S. T. Cundiff, Carrier-Envelope Phase Control of Femtosecond Mode-Locked Lasers and Direct Optical Frequency Synthesis, Science **288**, 635 (2000).

[9] S. G. Karshenboim, Precision physics of simple atoms: QED tests, nuclear structure and fundamental constants, Phys. Rep. **422**, 1 (2005).

[10] R. Pohl *et al.*, The size of the proton, Nature (London) **466**, 213 (2010).

[11] A. Antognini *et al.*, Proton structure from the measurement of $2S - 2P$ transition frequencies of muonic hydrogen, Science **339**, 417 (2013).

[12] R. Pohl, R. Gilman, G. A. Miller, and K. Pachucki, Muonic hydrogen and the proton radius puzzle, Annu. Rev. Nucl. Part. Sci. **63**, 175 (2013).

[13] A. Antognini *et al.*, Experiments towards resolving the proton charge radius puzzle, EPJ Web Conf. **113**, 01006 (2016).

[14] R. Pohl *et al.*, Laser spectroscopy of muonic deuterium, Science **353**, 669 (2016).

[15] H. Fleurbaey, S. Galtier, S. Thomas, M. Bonnaud, L. Julien, F. Biraben, F. Nez, M. Abgrall, and J. Guéna, New Measurement of the $1S - 3S$ Transition Frequency of Hydrogen: Contribution to the Proton Charge Radius Puzzle, Phys. Rev. Lett. **120**, 183001 (2018).

[16] N. Bezginov, T. Valdez, M. Horbatsch, A. Marsman, A. C. Vutha, and E. A. Hessels, A measurement of the atomic hydrogen Lamb shift and the proton charge radius, Science **365**, 1007 (2019).

[17] M. Herrmann *et al.*, Feasibility of coherent XUV spectroscopy on the $1S - 2S$ transition in singly ionized helium, Phys. Rev. A **79**, 052505 (2009).

[18] B. Franke, J. J. Krauth, A. Antognini, M. Diepold, F. Kottmann, and R. Pohl, Theory of the $n = 2$ levels in muonic helium-3 ions, Eur. Phys. J. D **71**, 341 (2017).

[19] M. Diepold, B. Franke, J. J. Krauth, A. Antognini, F. Kottmann, and R. Pohl, Theory of the Lamb Shift and fine structure in muonic $^4$He ions and the muonic $^3$He – $^4$He Isotope Shift, Ann. Phys. (Amsterdam) **396**, 220 (2018).

[20] L. von der Wense *et al.*, Direct detection of the $^{229}$Th nuclear clock transition, Nature (London) **533**, 47 (2016).

[21] L. von der Wense, B. Seiferle, S. Stellmer, J. Weitenberg, G. Kazakov, A. Pálffy, and P. G. Thirolf, A Laser Excitation Scheme for $^{229m}$Th, Phys. Rev. Lett. **119**, 132503 (2017).

[22] N. de Oliveira, M. Roudjane, D. Joyeux, D. Phalippou, J.-C. Rodier, and L. Nahon, High-resolution broad-bandwidth

Fourier-transform absorption spectroscopy in the VUV range down to 40 nm, Nat. Photonics **5**, 149 (2011).
[23] K. S. E. Eikema, W. Ubachs, W. Vassen, and W. Hogervorst, Precision Measurements in Helium at 58 nm: Ground State Lamb Shift and the $1^1S - 2^1P$ Transition Isotope Shift, Phys. Rev. Lett. **76**, 1216 (1996).
[24] P. B. Corkum, Plasma Perspective on Strong Field Multiphoton Ionization, Phys. Rev. Lett. **71**, 1994 (1993).
[25] M. Lewenstein, P. Balcou, M. Y. Ivanov, A. L'Huillier, and P. B. Corkum, Theory of high-harmonic generation by low-frequency laser fields, Phys. Rev. A **49**, 2117 (1994).
[26] R. Zerne, C. Altucci, M. Bellini, M. B. Gaarde, T. W. Hänsch, A. L'Huillier, C. Lyngå, and C.-G. Wahlström, Phase-Locked High-Order Harmonic Sources, Phys. Rev. Lett. **79**, 1006 (1997).
[27] M. Bellini, C. Lyngå, A. Tozzi, M. B. Gaarde, T. W. Hänsch, A. L'Huillier, and C.-G. Wahlström, Temporal Coherence of Ultrashort High-Order Harmonic Pulses, Phys. Rev. Lett. **81**, 297 (1998).
[28] C. Gohle, T. Udem, M. Herrmann, J. Rauschenberger, R. Holzwarth, H. A. Schuessler, F. Krausz, and T. W. Hänsch, A frequency comb in the extreme ultraviolet, Nature (London) **436**, 234 (2005).
[29] R. J. Jones, K. D. Moll, M. J. Thorpe, and J. Ye, Phase-Coherent Frequency Combs in the Vacuum Ultraviolet via High-Harmonic Generation inside a Femtosecond Enhancement Cavity, Phys. Rev. Lett. **94**, 193201 (2005).
[30] C. Benko, T. K. Allison, A. Cingöz, L. Hua, F. Labaye, D. C. Yost, and J. Ye, Extreme ultraviolet radiation with coherence time greater than 1*s*, Nat. Photonics **8**, 530 (2014).
[31] D. Z. Kandula, C. Gohle, T. J. Pinkert, W. Ubachs, and K. S. E. Eikema, Extreme Ultraviolet Frequency Comb Metrology, Phys. Rev. Lett. **105**, 063001 (2010).
[32] A. Cingöz, D. C. Yost, T. K. Allison, A. Ruehl, M. E. Fermann, I. Hartl, and J. Ye, Direct frequency comb spectroscopy in the extreme ultraviolet, Nature (London) **482**, 68 (2012).
[33] J. Morgenweg, I. Barmes, and K. S. E. Eikema, Ramsey-comb spectroscopy with intense ultrashort laser pulses, Nat. Phys. **10**, 30 (2014).
[34] J. Morgenweg and K. S. E. Eikema, Ramsey-comb spectroscopy: Theory and signal analysis, Phys. Rev. A **89**, 052510 (2014).
[35] N. F. Ramsey, A molecular beam resonance method with separated oscillating fields, Phys. Rev. **78**, 695 (1950).
[36] R. K. Altmann, S. Galtier, L. S. Dreissen, and K. S. E. Eikema, High-Precision Ramsey-Comb Spectroscopy at Deep Ultraviolet Wavelengths, Phys. Rev. Lett. **117**, 173201 (2016).
[37] R. K. Altmann, L. S. Dreissen, E. J. Salumbides, W. Ubachs, and K. S. E. Eikema, Deep-Ultraviolet Frequency Metrology of $H_2$ for Tests of Molecular Quantum Theory, Phys. Rev. Lett. **120**, 043204 (2018).
[38] C. Corsi, A. Pirri, E. Sali, A. Tortora, and M. Bellini, Direct Interferometric Measurement of the Atomic Dipole Phase in High-Order Harmonic Generation, Phys. Rev. Lett. **97**, 023901 (2006).
[39] A. Rundquist, C. G. Durfee III, Z. Chang, C. Herne, S. Backus, M. M. Murnane, and H. C. Kapteyn, Phase-matched generation of coherent soft X-rays, Science **280**, 1412 (1998).
[40] T. Popmintchev, M.-C. Chen, A. Bahabad, M. Gerrity, P. Sidorenko, O. Cohen, I. P. Christov, M. M. Murnane, and H. C. Kapteyn, Phase matching of high harmonic generation in the soft and hard X-ray regions of the spectrum, Proc. Natl. Acad. Sci. U.S.A. **106**, 10516 (2009).
[41] P. Salières, L. Le Déroff, T. Auguste, P. Monot, P. d'Oliveira, D. Campo, J.-F. Hergott, H. Merdji, and B. Carré, Frequency-Domain Interferometry in the XUV with High-Order Harmonics, Phys. Rev. Lett. **83**, 5483 (1999).
[42] Y.-H. Chen, S. Varma, I. Alexeev, and H. Milchberg, Measurement of transient nonlinear refractive index in gases using xenon supercontinuum single-shot spectral interferometry, Opt. Express **15**, 7458 (2007).
[43] J. Morgenweg and K. S. E. Eikema, Tailored pulse sequences from an 880 nm pumped $Nd:YVO_4$ bounce amplifier, Opt. Lett. **37**, 208 (2012).
[44] J. Morgenweg and K. S. E. Eikema, Multi-delay, phase coherent pulse pair generation for precision Ramsey-frequency comb spectroscopy, Opt. Express **21**, 5275 (2013).
[45] J. Wörmer, V. Guzielski, J. Stapelfeldt, and T. Möller, Fluorescence excitation spectroscopy of xenon clusters in the VUV, Chem. Phys. Lett. **159**, 321 (1989).
[46] A. Ozawa and Y. Kobayashi, VUV frequency-comb spectroscopy of atomic xenon, Phys. Rev. A **87**, 022507 (2013).
[47] W. F. Chan, G. Cooper, X. Guo, G. R. Burton, and C. E. Brion, Absolute optical oscillator strengths for the electronic excitation of atoms at high resolution. III. The photoabsorption of argon, krypton, and xenon, Phys. Rev. A **46**, 149 (1992).
[48] D. J. Armstrong, W. J. Alford, T. D. Raymond, A. V. Smith, and M. S. Bowers, Parametric amplification and oscillation with walkoff-compensating crystals, J. Opt. Soc. Am. B **14**, 460 (1997).
[49] K. Yoshino and D. E. Freeman, Absorption spectrum of xenon in the vacuum-ultraviolet region, J. Opt. Soc. Am. B **2**, 1268 (1985).
[50] M. Cadoret, E. De Mirandes, P. Cladé, F. Nez, L. Julien, F. Biraben, and S. Guellati-Khélifa, Atom interferometry based on light pulses: Application to the high precision measurement of the ratio h/m and the determination of the fine structure constant, Eur. Phys. J. Spec. Top. **172**, 121 (2009).